Optical properties of 4 Å-diameter single-walled nanotubes

M. Machón*, S. Reich*, J. Maultzsch*, P. M. Rafailov*, C. Thomsen*, D. Sánchez-Portal† and P. Ordejón**

*Institut für Festkörperphysik, Technische Universität Berlin, Hardenbergstr. 36, 10623 Berlin, Germany

†Centro Mixto CSIC-UPV/EHU and Donostia International Physics Center (DIPC), Apt. 1072, 20080 San Sebastián, Spain

**Institut de Ciència de Materials de Barcelona (CSIC), Campus de la U.A.B. E-08193 Bellaterra, Barcelona, Spain

Abstract.
We studied the electronic band structure and optical absorption of carbon nanotubes with small diameters ($d \approx 4$ Å), which grow in the channels of a zeolite crystal. The size of the channels determines the diameter of the nanotubes and restricts their possible chiralities to three [(3,3), (5,0), and (4,2)]. We performed *ab initio* calculations of the electronic band structure and optical absorption of the mentioned nanotubes. We discuss our results and compare them with optical and Raman data.

The recent development of samples of aligned single walled nanotubes with a diameter of ≈ 4 Å[1] has attracted the interest of many research groups. The narrow diameter distribution and small size of the nanotubes present in the sample allow exhaustive *ab initio* studies of their properties. Furthermore, the alignment of the nanotubes makes polarization dependent measurements possible.

We present *ab initio* density functional theory calculations for the (3,3), (5,0) and (4,2) nanotubes [2], performed with the SIESTA code [3, 4] within the local density approximation, as parametrized by Perdew and Zunger.[5] The core electrons were replaced by non-local norm-conserving pseudopotentials. [6] A double-ζ, singly polarized basis set of localized atomic orbitals was used for the valence electrons, with cutoff radii of 5.12 a.u. for the s and 6.25 a.u. for the p and d orbitals as determined from an energy shift of 50 meV by localization [7, 8]. In the directions perpendicular to the tube axis a unit cell of side 9 Å was used in order to minimize the interaction among the images.

First, the electronic band structure was calculated, the most interesting feature being the metallic character of the (5,0) nanotube. This effect, contrary to the prediction of the zone folding approximation was found by Blase *et al.* [9] to be a consequence of the increasing curvature of the nanotube walls for decreasing radius. The (3,3) nanotube is metallic, and the (4,2) semiconducting.

Using the band structures, the dielectric function of the three nanotubes was calculated for incident light polarized both parallel and perpendicular to the nanotube axis. The effect of the arbitrary size of the unit cell was taken into account, using the expression

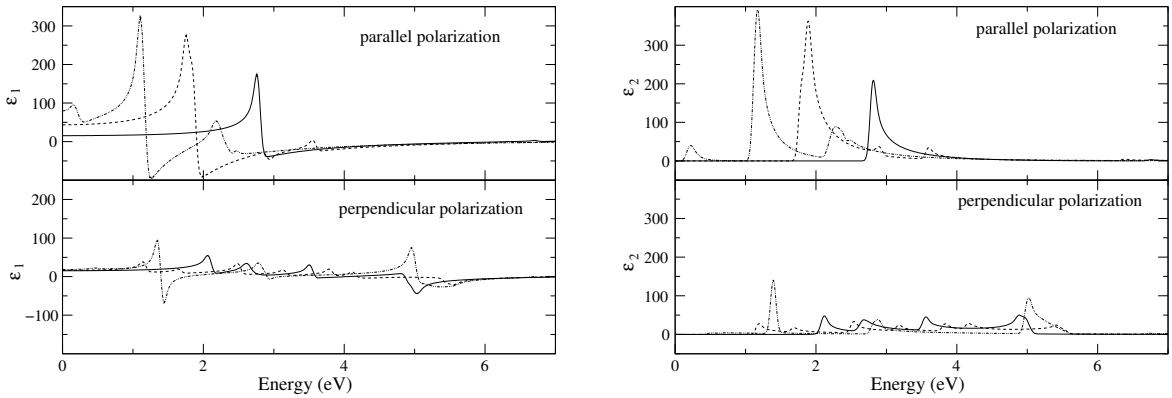

FIGURE 1. Dielectric function of the three isolated nanotubes. Left: real part, right: imaginary part. The solid line corresponds to the (3,3) nanotube, the dotted line to the (5,0), and the dashed line to the (4,2).

$\varepsilon_{\mathrm{NT}} = \frac{V_{\mathrm{SC}}}{V_{\mathrm{NT}}}\varepsilon_{\mathrm{SC}}$ where $\varepsilon_{\mathrm{SC}}$ is the calculated imaginary part of the dielecric function, $\varepsilon_{\mathrm{NT}}$ the dielectric function of the nanotube, V_{SC} is the volume of the unit cell for the *ab initio* calculation, and V_{NT} the volume that the nanotubes occupy in the zeolite channel.

The results, shown in Fig. 1 are strongly anisotropic. Comparing the upper and lower panels of each Figure, we see how the energy range of the finite response is wider for perpendicular than for parallel polarization whereas the intensity becomes lower.

To be able to compare our results with experimental data, the effect of the embedding zeolite must be taken into account. Since we are interested in the long-wavelength range, we can treat the medium as homogeneous and use an effective dielectric function [10]. For the polarization parallel to the tube axis, the effective dielectric function can be calculated as a volume-weighted average of the components

$$\varepsilon_{\mathrm{eff}}(\omega) = \frac{f[\varepsilon_{(3,3)} + \varepsilon_{(5,0)} + \varepsilon_{(4,2)}]}{3} + (1-f)\varepsilon_{\mathrm{zeol}} \tag{1}$$

where f, the filling fraction of the nanotubes, is defined as

$$f = \frac{\pi R^2}{a^2 \cos 30^\circ}. \tag{2}$$

$a = 1.37\,\mathrm{nm}$ is the distance between the centers of two adjacent channels in the zeolite crystal, and R is the radius of the zeolite channels. The concentration of the three chiralities was assumed to be homogeneous. The dielectric function of the zeolite was calculated from the measurements of the index of refraction by Striebel *et al.* [11] using the Kramers-Kronig relations.

In Fig. 2a the calculated effective optical absorption of the zeolite-nanotubes composite can be seen. It can be compared with the measurements of the optical density performed by Li *et al.* [12] (Fig 2b). The agreement in the position of the maxima is

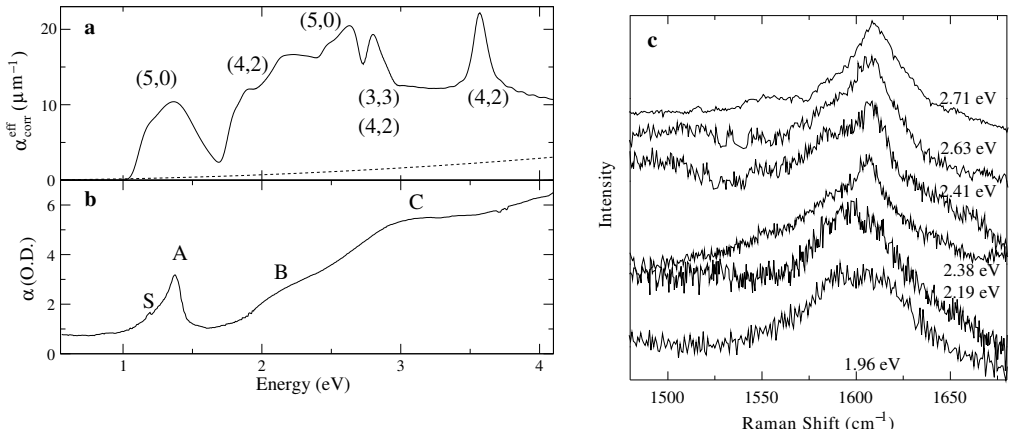

FIGURE 2. a) Solid line: effective optical absorption of the zeolite-nanotubes composite under light polarized parallel to the nanotube axis corrected with the effective reflectance. Dashed line: optical absorption of empty zeolite. Next to the peaks are the corresponding chiralities according to our calculations obtained comparing $\alpha_{\rm corr}^{\rm eff}$ with the absorption of the isolated nanotubes. b) Optical absorption of the zeolite-nanotube composite under light polarized parallel to the nanotube axis measured by Li *et al.* (Ref. [12]) who identified a shoulder (S) and three peaks (A,B and C). c) Raman spectra of nanotubes embedded in zeolite for different excitation energies (indicated next to the spectra).

excellent within the error of $\approx$ 10-20% reported by Li *et al.* [12] and Reich *et al.* [13], intrinsic to LDA calculations. We are able not only to reproduce the features of the observed absorption spectra, but also to assign these features to individual chiralities. In Table 1 the experimental positions of the optical absorption maxima are shown, aligned with the corresponding calculated optical transition energies of the nanotubes.

The calculated peak between 1 and 1.5 eV iv Fig 2a has a low energy shoulder, very similar as in the experimental espectra. Interestingly, this apparent double-peak structure arises only from a simple maximum in the optical absorption coefficient [1.2 eV transition of the (5,0) nanotube]. The shoulder to lower energies results from the reflectivity correction, which supresses the square root singularity at 1.2 eV and thus shifts the transmission peak to higher energies. Another interesting point is the strong absorption peak of the (4,2) nanotube at 3.6 eV predicted theoretically, which is absent in the experimental spectra. Recent experimental studies indicate a lower concentration of (4,2) than (5,0) and (3,3) [14]. This would lower the peaks corresponding to the (4,2) nanotube, yielding an even better agreement between theory and experiment.

A series of energy dependent Raman measurements was performed on the nanotube filled zeolite samples as shown in Fig. 2c. The measured Raman intensity depends, among other factors, on the optical absorption of the samples. After normalizing the data with respect to laser intensity and detector sensitivity, we observed an increase of the intensity of the peak at 1610 $\rm cm^{-1}$ towards higher excitation energies. This tendency agrees nicely with the measured increase in the absorption in the same energy range.

Summarizing, we performed *ab initio* calculations of the electronic and optical properties of the (3,3), (5,0) and (4,2) nanotubes. A simple model was used to obtain an

TABLE 1. Energies in eV of the experimental optical absorption maxima of the SWNT containig zeolite and the calculated optical transition energies.

	S	**A**	**B**	**C**
Exp.(Ref. [12])	1.2	1.37	2.1	3.1
(3,3)				2.9
(5,0)		1.2	2.4	
(4,2)			1.9	3.0-3.6

effective optical absorption of the mentioned nanotubes embedded in zeolite. These results were compared with transmission measurements performed by Li *et al.* [12]. We assigned the experimentally observed maxima to the three distinct tubes present in the zeolite crystal. Energy dependent Raman spectroscopy was performed on the zeolite-nanotubes samples, and found to agree nicely with the optical data.

ACKNOWLEDGMENTS

We acknowledge the Ministerio de Ciencia y Tecnología (Spain) and the DAAD (Germany) for a Spanish-German Research action (HA 1999-0118). P. O. acknowledges support from Fundación Ramón Areces (Spain), EU project SATURN IST-1999-10593, and Spain-DGI project BMF2000-1312-002-01.

REFERENCES

1. Wang, N., Li, G. D., and Tang, Z. K., *Chem. Phys. Lett.*, **339**, 47 (2001).
2. Machón, M., Reich, S., Thomsen, C., Sánchez-Portal, D., and Ordejón, P. (Submitted to Phys. Rev. B).
3. Sanchez-Portal, D., Ordejón, P., Artacho, E., and Soler, J. M., *Int. J. Quantum Chem.*, **65**, 453 (1997).
4. Soler, J. M., Artacho, E., Gale, J. D., García, A., Junquera, J., Ordejón, P., and Sánchez-Portal, D., *J. Phys. Condens. Mat.*, **14**, 2745 (2002).
5. Perdew, J. P., and Zunger, A., *Phys. Rev. B*, **23**, 5048 (1981).
6. Troullier, N., and Martins, J., *Phys. Rev. B*, **43**, 1993 (1991).
7. Junquera, J., Paz, O., Sánchez-Portal, D., and Artacho, E., *Phys. Rev. B*, **64**, 235111 (2001).
8. Artacho, E., Sánchez-Portal, D., Ordejón, P., García, A., and Soler, J., *phys. stat. sol. (b)*, **215**, 809 (1999).
9. Blase, X., Benedict, L. X., Shirley, E. L., and Louie, S. G., *Phys. Rev. Lett.*, **72**, 1878 (1994).
10. Pitarke, J. M., and García-Vidal, F. J., *Phys. Rev. B*, **63**, 073404 (2001).
11. Striebel, C., Hoffmann, K., and Marlow, F., *Microporous Materials*, **9**, 43 (1997).
12. Li, Z. M., Tang, Z. K., Liu, H. J., Wang, N., Chan, C. T., Saito, R., Okada, S., Li, G. D., Chen, J. S., Nagasawa, N., and Tsuda, S., *Phys. Rev. Lett.*, **87**, 127401 (2001).
13. Reich, S., Thomsen, C., and Ordejón, P., *Phys. Rev. B*, **65**, 155411 (2002).
14. Tang, Z. K. (Private communication).